

---

Konrad-Zuse-Zentrum für Informationstechnik Berlin  
Heilbronner Str. 10, D-10711 Berlin - Wilmersdorf

H. Niemann, D. Schmidt, U. Maas

**An Efficient Storage Scheme for Reduced Chemical Kinetics  
Based on Orthogonal Polynomials**

# An Efficient Storage Scheme for Reduced Chemical Kinetics Based on Orthogonal Polynomials

H. Niemann, D. Schmidt

Interdisziplinäres Zentrum für Wissenschaftliches Rechnen, Universität Heidelberg  
Im Neuenheimer Feld 368, 69120 Heidelberg, Germany

U. Maas

Konrad-Zuse-Zentrum für Informationstechnik  
Heilbronner Str. 10, 10711 Berlin, Germany

May 23, 1996

## Abstract

Simplified chemical kinetic schemes are a crucial prerequisite for the simulation of complex three-dimensional turbulent flows, and various methods for the generation of reduced mechanisms have been developed in the past. The method of intrinsic low-dimensional manifolds (ILDM), e.g., provides a mathematical tool for the automatic simplification of chemical kinetics, but one problem of this method is the fact that the information which comes out of the mechanism reduction procedure has to be stored for subsequent use in reacting flow calculations. In most cases tabulation procedures are used which store the relevant data (such as reduced reaction rates) in terms of the reaction progress variables, followed by table look-up during the reacting flow calculations. This can result in huge amounts of storage needed for the multi-dimensional tabulation. In order to overcome this problem we present a storage scheme which is based on orthogonal polynomials. Instead of using small tabulation cells and local mesh refinement, the thermochemical state space is divided into a small number of coarse cells. Within these coarse cells polynomial approximations are used instead of frequently used multi-linear interpolation. This leads to a considerable decrease of needed storage. The hydrogen-oxygen system is considered as an example. Even for this small chemical system we obtain a decrease of the needed storage requirement by a factor of 100.

# 1 Introduction

The interest in the numerical simulation of reacting flows has grown considerably during the last years. The underlying chemical kinetics of combustion processes is (at least for aliphatic hydrocarbons) adequately well understood [1], and numerical methods are available, which allow to couple chemical kinetics with flow and molecular transport. Numerical simulations of laminar flames in one- or two-dimensional configurations have become a standard tool in combustion research (see, e.g. [2, 3]). However, if one is interested in general, multi-dimensional, turbulent flames, a detailed treatment of the chemical and physical processes is, and will be in the near future, computationally prohibitive [4]. Thus, simplified models for the turbulence (see, e.g., [4–6]), as well as for the chemical kinetics have to be devised.

The need of simplified models for the chemistry stems from the fact that for each chemical species (which can be more than 1000 in the low-temperature oxidation of higher hydrocarbons [7]) a species conservation equation has to be solved. This is possible, if simple systems like spatially homogeneous ignition (e.g. in shock tubes) are simulated [1], but computationally prohibitive for other reacting flows.

Almost 100 years ago Bodenstein [8] observed that some chemical reactions are so fast that some chemical species in the reaction system are in a quasi-steady state. Based on the ideas of Bodenstein, many attempts have been made to develop simplified descriptions of chemical reaction systems, e.g., for the simulation of complex combustion processes. A variety of different approaches can be found in the literature, such as systematically reduced mechanisms [9], the constrained equilibrium approach [10], computational singular perturbation [11, 12], repro-modelling [13], dynamic dimension reduction [14], or the method of intrinsic low-dimensional manifolds [15–17], to name only a few examples. Good surveys of current work can be found in [9, 18, 19]. In this work we shall present some new results of the implementation of reduced chemistry based on intrinsic low-dimensional manifolds (ILDm).

The scalar field of a reacting flow involving  $n_s$  species evolves in time according to an  $(n_\psi = n_s + 2)$ -dimensional partial differential equation system

$$\frac{\partial \underline{\psi}}{\partial t} = \underline{F}(\underline{\psi}) + \underline{\Xi}(\underline{\psi}, \nabla \underline{\psi}, \nabla^2 \underline{\psi}). \quad (1)$$

In this equation  $\underline{\psi} = (h, p, w_1/M_1, w_2/M_2, \dots, w_{n_s}/M_{n_s})^T$  denotes the vector of scalars with  $h$ =specific enthalpy,  $p$ =pressure,  $M_i$  the molar mass and  $w_i$  the mass fraction of the species  $i$ .  $\underline{F}(\underline{\psi})$  denotes the vector of chemical reaction rates, and  $\underline{\Xi}(\underline{\psi}, \nabla \underline{\psi}, \nabla^2 \underline{\psi})$  the vector describing all the physical processes, such as convection, diffusion, heat conduction, etc..

The ILDM-approach [15, 16], as well as all the other approaches, uses the fact that in typical reaction systems a large number of chemical processes are so fast that they are not rate limiting and can be decoupled. All the method does is to identify intrinsic low-dimensional manifolds in the  $(n_\psi = n_s + 2)$ -dimensional state space with the property that after a short relaxation time the thermochemical state of the system has relaxed onto these attracting low-dimensional manifolds. Then the state of the chemical system is a known function of only a few  $N$  variables  $\underline{\theta}$  which parameterize the manifold, i.e.  $\underline{\psi} = \underline{\psi}(\underline{\theta})$ , and the governing  $n_\psi$ -dimensional equation system (1) can be projected onto the  $N$ -dimensional subspace

$$\frac{\partial \underline{\theta}}{\partial t} = \underline{S}(\underline{\theta}) + \underline{\Gamma}(\underline{\theta}, \nabla \underline{\theta}, \nabla^2 \underline{\theta}). \quad (2)$$

Thus, the ILDM-approach basically consists of three steps [15–17, 20]:

- Identify the ILDM and obtain information about the coupling of the chemical kinetics with flow and molecular transport.
- Store the information, namely  $\underline{\psi}(\underline{\theta})$  and the projection  $\underline{\Xi} \rightarrow \underline{\Gamma}$  for subsequent use in the reacting flow simulation.
- Solve the projected partial differential equation system (2) for the scalar field.

Various examples have been treated and they have verified the approach [17,20–24]. It turns out that the main remaining challenges in the implementation of the method are

- The efficient numerical calculation of the ILDM.
- A local adaption of the dimension of the manifolds based on the desired accuracy of the reduced scheme.
- The efficient storage of all the data needed for the subsequent use in the reacting flow calculation.

In this paper we address the third item, namely an efficient storage of the ILDM.

## 2 Polynomial Storage Scheme

### 2.1 Problem Formulation

The implementation of ILDM-reduced chemistry in CFD-codes is based on the projection of the  $n_\psi$ -dimensional conservation equations for the scalar field onto the  $N$ -dimensional attracting ILDM. This procedure requires the knowledge of several properties of the reduced scheme, namely

- $N$  rates  $\underline{S}(\underline{\theta})$  for the reduced variables,
- the  $n_\psi$  state variables  $\underline{\psi}(\underline{\theta})$  characterizing the manifold,
- and  $N \times n_\psi$  entries of the projection operator  $P(\underline{\theta})$  which describes the coupling of the chemistry with the physical processes.

Because the evaluation of the ILDM is quite time consuming, and the results are usually used in a large number of different CFD-calculations, the properties given above are usually calculated beforehand and stored in terms of the reduced state variables  $\underline{\theta}$ .

The storage scheme for the ILDM used up to now was based on a table set-up procedure [16]. The tabulation region was predefined and an adaptive grid with local mesh refinement was used (see Fig. 1). Within the grid cells multi-linear interpolation was used to calculate the properties from the values at the grid nodes. The disadvantage of this storage scheme is the huge size of these tables for future applications. If one is thinking of modelling real diesel engine combustion, at least 3 reaction progress variables are needed. Additionally the parameters pressure, enthalpy and mixture fraction have to be varied as tabulation coordinates, leading to a table with tabulating dimension at least  $N = 6$ . Considering about 1000 species taking part in the reactions and at least 10 grid points in each tabulation direction one ends up with about  $10^9$  numbers to be stored. This table can not be handled. The problem gets worse, if we account for differential diffusion, adding element composition variables to the set of reduced variables. From this it can be seen that an efficient storage of

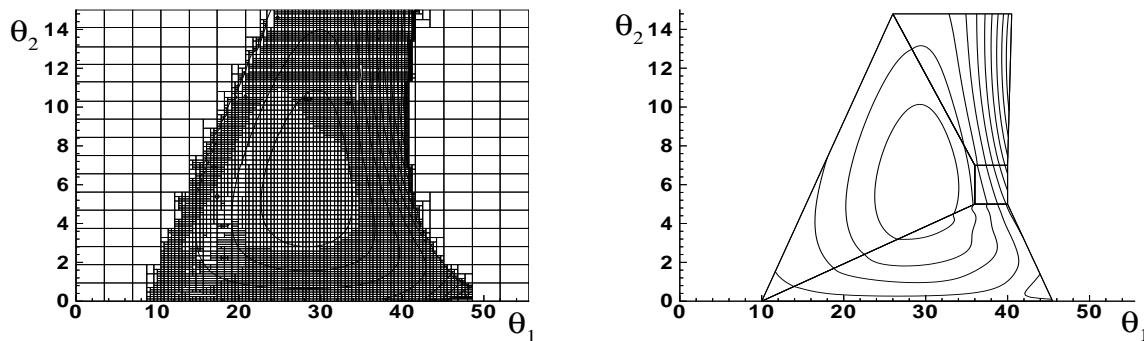


Figure 1: Different grid-types, isolines denote equal rates of formation of  $\text{H}_2\text{O}$ . (Left: Conventional storage scheme, Right: New storage scheme with coarse cells)

the reduced mechanism is crucial for its use in CFD-codes, and several approaches alternative to the tabulation have been pursued (see, e.g., [13, 25, 26]).

We start the development of our storage procedure based on two observations:

- It is evident that, if we replace the multi-linear interpolation in the grid cells by higher order polynomial, the accuracy is improved considerably.
- If we use the tabulation procedure outlined above [16], it is inevitable that the refinement is based on all the different properties which have to be stored. Thus, the property with the worst local behavior is defining the local grade of refinement though all other properties might have a smooth behavior. A solution to overcome this is to use different interpolating functions for each property with adaptive complexity and order.

Multidimensional polynomials are the most simple functions to use. They can be evaluated efficiently with Horner schemes. The idea using polynomials for approximation of chemical reaction rate data is shown in [25]. An overview of the literature can be found there, too. However, this approach has some disadvantages: The use of only one polynomial for the whole tabulation domain usually requires a very high order of the polynomial. This will lead to numerical problems in every fitting algorithm. If this problem is circumvented by dividing the tabulation domain into sub-domains and fitting the different sub-domains with own low-grade polynomials, the properties are not continuous at the cell boundaries. This leads to problems in using the table in CFD-codes, especially when gradient based solvers are used.

In order to overcome these deficiencies, we develop a procedure, which divides the whole state space into sub-domains, uses medium-grade polynomials within these sub-domains, and additionally ensures continuity at the boundaries of the sub-domains. The approximating polynomials are computed independently for each cell. That enhances the flexibility of the table setup and enables a parallelization of the tabulation code.

## 2.2 Coarse Grid and Local Coordinates

Let us start the analysis with a brief survey of the nomenclature that we have adopted. The manifold is given as a subset  $\mathcal{M}$  of the state space with

$$\mathcal{M} = \{\underline{\psi}(\underline{\theta}) | \theta \in \mathcal{D}\}, \quad (3)$$

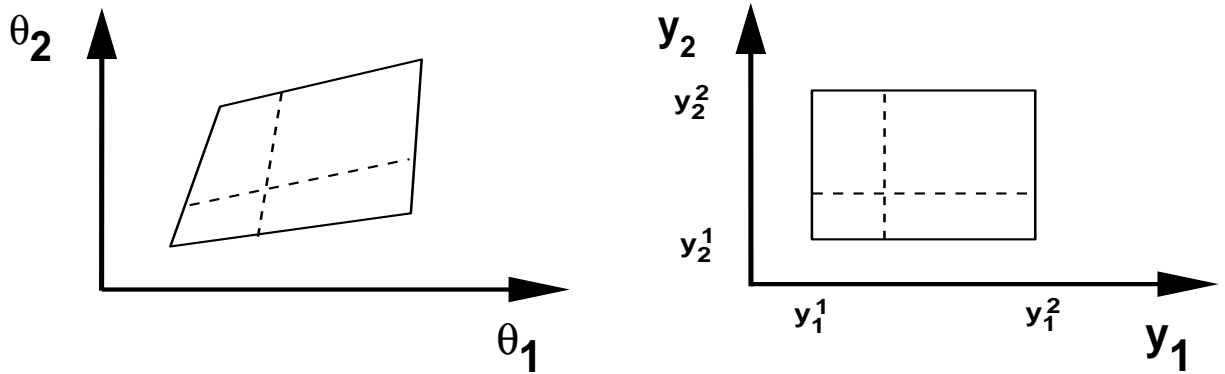


Figure 2: Transformation from global coordinates to local cell-coordinates.

where  $\underline{\theta} \rightarrow \underline{\psi}$  defines the mapping of the reduced variables onto the respective points of the manifolds, and  $\mathcal{D}$  defines the domain of the reduced variables. The mappings  $\underline{\theta} \rightarrow \underline{\psi}$  and  $\underline{\psi} \rightarrow \underline{\theta}$ , as well as the domain  $\mathcal{D}$  are obtained during the generation of the ILDM. This will be the topic of another publication. In the following we assume explicitly that the mapping (the parameterization of the manifold) as well as  $\mathcal{D}$  are known. Thus, in order to simplify the presentation, we start from a given manifold which has been obtained using a tabulation procedure [16]. As an example we use the ILDM of a hydrogen-oxygen system. The two-dimensional manifold is parameterized in terms of two reaction progress variables  $\theta_1 = w_{\text{H}_2\text{O}}/M_{\text{H}_2\text{O}}$  and  $\theta_2 = w_{\text{H}}/M_{\text{H}}$  which are in the intervals  $0 < \theta_1 < \theta_1^{\text{max}}$  and  $0 < \theta_2 < \theta_2^{\text{max}}$ . The conventional tabulation of the manifold is shown in the left part of Figure 1. For an efficient storage of the ILDM we divide this domain into sub-domains as it can be seen in the right part of Figure 1. For simplicity of the table lookup it was decided to use coarse cells that can be mapped on rectangular cells. So the coarse cells have always  $2^N$  corners ( $N$  is the tabulation-dimension). The choice of the coarse cells can, of course, be guided by the information coming out of the mechanism reduction procedure. For the example considered here we base the set-up of the coarse cells on the known behavior of the reaction rates (cf. Fig. 1). Having specified the coarse cells, the local coordinates in each cell are established by the mapping  $\underline{\theta} \rightarrow \underline{y}$  of the cell on a rectangular cell with the coordinates  $\underline{y}$ , as it can be seen in Figure 2. The cell is bounded by the cell coordinates  $y_i^1$  and  $y_i^2$ ,  $i = 1, 2, \dots, N$ , and the cell is given by  $\mathcal{S}^N = \{ \underline{y} | y_i \in [y_i^1, y_i^2], i = 1, 2, \dots, N \}$ . The choice of the local corner coordinates  $(y_i^1, y_i^2)$  is arbitrary in the mapping aspect.

The remaining task is now to find a polynomial representation of  $\underline{S}(\underline{\theta})$ ,  $\underline{\psi}(\underline{\theta})$  and  $P(\underline{\theta})$  within the coarse cells with the additional constraint that the functions are continuous over the cell boundaries.

## 2.3 Polynomial Interpolation within the Coarse Cells

### 2.3.1 Ensuring Continuous Functions at the Boundaries

The idea behind making continuous functions between two neighbouring cells is to calculate a function on the shared boundary first, and then to use this boundary function for the calculation of the approximating function (cell-function) within the cell. On the boundary the cell function is forced to degenerate to the boundary function. For the two-dimensional example shown in Figure 1 this means calculating functions on the straight border lines first, and then fitting the area inside the cells.

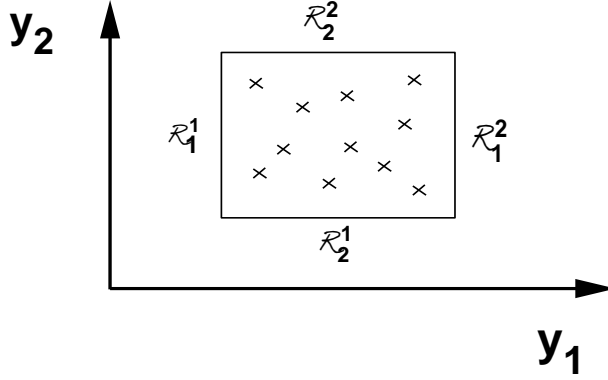


Figure 3: Cell with a set of reference points inside and boundary functions  $b_i^j(\underline{y})$  on the boundaries  $\mathcal{R}_i^j$ .

Given an  $N$ -dimensional cell  $\mathcal{S}^N$ , we have  $2N$  bounding hyperplanes  $\mathcal{S}_i^{N-1}$ ,  $i = 1, 2, \dots, 2N$ , which shall be denoted by  $\mathcal{R}_i^j = \{\underline{y} | \underline{y} \in \mathcal{S}^N \wedge y_i = y_i^j\}$ ,  $i = 1, 2, \dots, N$ , and  $j = 1, 2$ . On the bounding hyperplanes ( $\underline{y} \in \mathcal{R}_i^j$ ) the approximating functions shall be given by  $b_i^j(\underline{y})$ . In the cell the following ansatz is used for the approximating function  $F(\underline{y})$ :

$$F(\underline{y}) = Z(\underline{y})L(\underline{y}) + B(\underline{y}). \quad (4)$$

On the boundaries  $\mathcal{S}_i^{N-1}$  the function  $Z(\underline{y})$  is forced to equal Zero

$$Z(\underline{y}) = \prod_{i=1}^N (y_i - y_i^1)(y_i - y_i^2). \quad (5)$$

There the ansatz (4) degenerates to  $F(\underline{y}) = B(\underline{y})$ . By defining the boundary function  $B(\underline{y})$  such that  $B(\underline{y}) = b_i^j(\underline{y})$  for all  $\underline{y}$  in  $\mathcal{R}_i^j$ , continuity between cells is ensured. The calculation of  $B(\underline{y})$  is a bit tricky. It is based on the condition that the polynomials of  $b_i^j(\underline{y})$  do not contain any powers of  $y_i$  together with the condition that  $B(\underline{y}) = b_i^j(\underline{y})$  for all  $\underline{y}$  in  $\mathcal{R}_i^j$ . From this a recursion formula for the coefficients of the monomials can be obtained. The fitting in the interior cell is done by a serial expansion of  $L(\underline{y})$  under the above constraints, so that the approximation error between  $F(\underline{y})$  and some reference points from the ILDM is kept below a given limit.

### 2.3.2 Calculation of the Approximating Polynomials

The function  $L(\underline{y})$  is calculated in a least-square-sense minimizing the relative error between  $F(\underline{y})$  and a set of reference points calculated inside the cell. Due to the previous calculation of  $B(\underline{y})$  and its linear interpolation property less effort has to be taken in the least-square step. This is especially helpful for the application on ILDM-tables, because the evaluation of points on the manifold is quite expensive, and the needed number of reference points to be calculated should be as small as possible.

The aim in calculating  $L(\underline{y})$  is to reduce the average relative error between the function  $F(\underline{y})$  and the values  $p^{(i)}(\underline{y})$  at the  $m$  reference points  ${}^i\underline{y}$  below a given limit  $\epsilon$

$$\sum_{i=1}^m \left( \frac{F({}^i\underline{y}) - p^{(i)}({}^i\underline{y})}{p^{(i)}({}^i\underline{y})} \right)^2 < m\epsilon^2. \quad (6)$$

This is achieved by a serial expansion of  $L(\underline{y})$ . For this the following ansatz is used:

$$L(\underline{y}) = \sum_{j=1}^k a_j \phi_j(\underline{y}). \quad (7)$$

Here  $\phi_j(\underline{y})$  are the basis functions for the series. The  $a_j$  are coefficients that have to be adjusted in the least-square step.

Introducing the serial expansion (7) into the ansatz (4) combined with the condition of minimizing the sum of the squared relative errors (6) leads to the following linear system of equations to determine the  $k$  unknown coefficients  $a_l$

$$\begin{aligned} \sum_{j=1}^k a_j \sum_{i=1}^m \left( \frac{B(\underline{i}\underline{y})}{p(\underline{i}\underline{y})} \right)^2 \phi_j(\underline{i}\underline{y}) \phi_l(\underline{i}\underline{y}) \\ + \sum_{i=1}^m \left( \frac{B(\underline{i}\underline{y})}{p(\underline{i}\underline{y})} - 1 \right) \frac{Z(\underline{i}\underline{y})}{p(\underline{i}\underline{y})} \phi_l(\underline{i}\underline{y}) = 0 \quad l = 1 \dots k. \end{aligned} \quad (8)$$

In the above form all  $k$  equations are coupled. A real expansion of the series in the sense of calculating all  $a_l$  independently one by one, until the required accuracy is achieved, seems to be computationally prohibitive. But defining a scalar product by

$$\langle \phi_j, \phi_l \rangle = \sum_{i=1}^m \left( \frac{B(\underline{i}\underline{y})}{p(\underline{i}\underline{y})} \right)^2 \phi_j(\underline{i}\underline{y}) \phi_l(\underline{i}\underline{y}) \quad (9)$$

and choosing the basis functions orthonormal according to this definition, the linear equation system (8) is diagonalized and the coefficients  $a_l$  can be calculated independently by

$$a_l = \sum_{i=1}^m \left( 1 - \frac{B(\underline{i}\underline{y})}{p(\underline{i}\underline{y})} \right) \frac{Z(\underline{i}\underline{y})}{p(\underline{i}\underline{y})} \phi_l(\underline{i}\underline{y}), \quad (10)$$

until the accuracy is high enough.

The coefficients to build the basis functions  $\phi_j(\underline{y})$  from the monomials  $(1, y_1, y_2, \dots, y_N, y_1^2, y_1 y_2, y_2^2, \dots, y_N^2, y_1^3, \dots)$  are calculated in parallel to the expansion of the series  $L(\underline{y})$  by the Gram-Schmidt-orthogonalization [27]. The well known instability of the Gram-Schmidt process is not crucial in this application because instead of calculating high order polynomials the size of the coarse cells is reduced, resulting in a smaller number of necessary basis functions that have to be orthogonalized. At this point it turns to be out, that it is numerically advantageous to choose the local coordinates in range from  $-1$  to  $1$  in each dimension.

Another advantage of this scheme is the high amount of freedom in choosing the reference points  $p(\underline{i}\underline{y})$  to adjust the approximating polynomial. In principal no regular pattern is needed, as it is sketched in Figure 3. If there are numerical problems in calculating a reference point at some local coordinates  $\underline{i}\underline{y}$  (e.g. a point may be outside of the range of existence of the manifold), this point  $p(\underline{i}\underline{y})$  can be rejected without any problem. But for a reliable outcome of the approximation a homogeneous distribution of reference points should be achieved. In the current implementation, the sample points  $p(\underline{i}\underline{y})$  are calculated on regular meshes as it can be seen in Figure 4. The first point to be calculated is the one in the middle of the cell. By this,  $2^N$  sub-cells are defined. The next points to be calculated are the

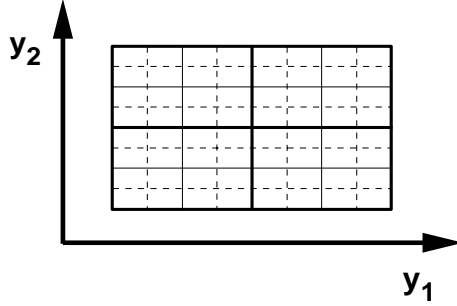


Figure 4: Grid of reference points with 3 levels of refinement.

mid-points of these sub-cells. This process of defining minor sub-cells and evaluation of mid-points can be continued until there are sufficient reference points. The number of calculated reference points  $m$  is adjusted automatically to the number of used monomials  $k$ . In this way unphysical waves and oscillations in the approximating polynomial can be avoided. In the current implementation the grid is refined one level by calculation of additional points, when  $m < 3k$ . After calculating the coefficients of  $B(\underline{y})$ ,  $Z(\underline{y})$  and  $L(\underline{y})$  they form one resulting polynomial  $F(\underline{y})$ . These coefficients are tabulated.

### 2.3.3 Calculation of the Boundary-Element-Functions

Up to this point the calculation of the boundary-element-functions  $b_i^j(\underline{y})$  was still not mentioned. They are calculated by the same algorithm according to ansatz (4) in one lower dimension. There the same problem of the sub-element boundary functions does arise. Each  $N$ -dimensional cell has  $\sigma_N^i$   $i$ -dimensional boundaries  $\mathcal{S}_j^i$  ( $j = 1, 2, \dots, \sigma_N^i$ ), where

$$\sigma_N^i = \frac{N!}{i!(N-i)!} 2^{N-i}. \quad (11)$$

Thus, a 2-dimensional cell has  $\sigma_2^0 = 4$  corner points and  $\sigma_2^1 = 4$  bounding edges, a 3-dimensional cell has  $\sigma_3^0 = 8$  corner points,  $\sigma_3^1 = 12$  bounding edges, and  $\sigma_3^2 = 6$  bounding surfaces. For the set-up of the boundary functions we perform a sweep through the dimensions (see Fig. 5):

1. Start with the  $\sigma_N^0$  corner points  $\mathcal{S}_j^0$  of the cell, and use the values as boundary-element functions to calculate the approximating functions on the  $\sigma_N^1$  bounding edges  $\mathcal{S}_j^1$ .
2. Use the approximating functions on these bounding edges as boundary functions to calculate the approximating functions on the the  $\sigma_N^2$  bounding surfaces  $\mathcal{S}_j^2$ .
3. Continue this process until the approximating function in the cell ( $\sigma_N^N$ ) has been calculated from the boundary functions defined by the approximating functions on the hyperplanes ( $\sigma_N^{N-1}$ ).

## 3 Application to the ILDM of a Stoichiometric H<sub>2</sub>-O<sub>2</sub> system

The new tabulation method shall now be demonstrated and verified using the ILDM of a stoichiometric hydrogen-oxygen system [17]. In this example 52 properties are tabulated in terms of two reaction progress variables ( $\theta_1 = w_{\text{H}_2\text{O}}/M_{\text{H}_2\text{O}}$ ,  $\theta_2 = w_{\text{H}}/M_{\text{H}}$ ). The setup of the

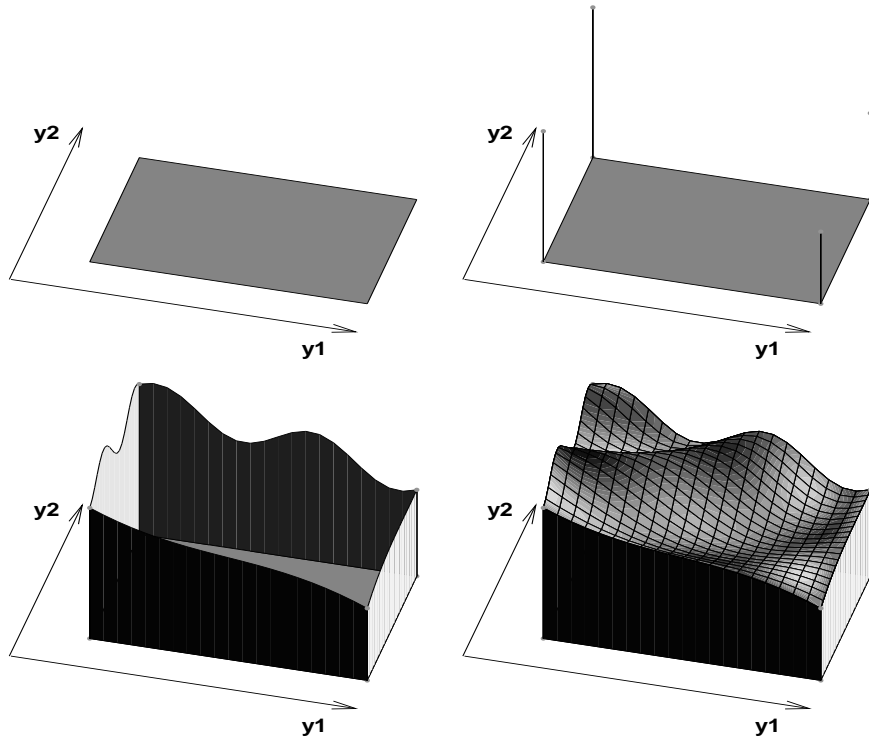


Figure 5: Idea of fitting algorithm in a two-dimensional example: 1) Setup of rectangular domain. 2) Evaluation of the values at the corners of the cell. 3) Fitting of the one-dimensional boundaries of the two-dimensional domain. 4) Fitting of the two-dimensional inner area of the cell.

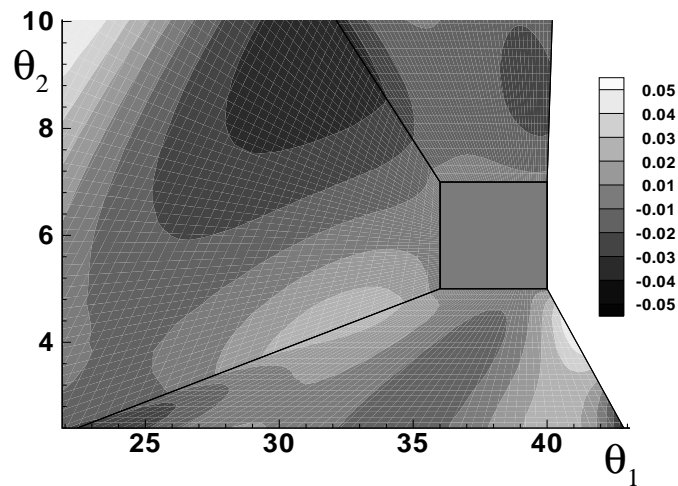


Figure 6: Relative approximation error for the mass fractions of OH radicals for the ILDM of a stoichiometric  $\text{H}_2\text{-O}_2$ -system.

coarse grid has been done by hand. A small cell has been inserted near the equilibrium value to allow a high resolution of the reaction rates near the equilibrium. (cf. Fig 1). The error tolerance (average relative error) for the fitting procedure was set to 0.05. Having in mind the usual uncertainty of kinetic data, this accuracy is high enough for practical calculations. But of course the accuracy can be increased if necessary. The grade of the approximating polynomial is adapting automatically to match the desired accuracy. For this application the resulting grade changes from constant monomials up to grade 5 polynomials. Most properties are fitted by grade 3 polynomials.

In Figure 6 the relative approximation errors for the mass fractions of OH-radicals are shown as contours. The small cell contains the domain around the chemical equilibrium where enhanced accuracy is needed. It can be seen, that the equilibrium region is approximated with high accuracy. This is desirable for the application in CFD-codes due to the high sensitivity of the CFD-results on the used chemistry near the equilibrium value. Furthermore it can be seen from Fig. 6 that the relative error at the cell-boundaries is continuous and vanishes at the cell corners. By this it is shown that the algorithm produces fitting polynomials with the desired continuity between the cells. In addition Figure 6 shows the smooth and well behaved property of the fitting. The highest relative errors are in the range of the predefined average error tolerance and no artificial oscillations (known from simple polynomial approximations) are produced. This is expected, because a least-square approach with much more reference points than coefficients to be fitted is used.

The computing time for the polynomial storage scheme is in the range of a few minutes. Compared to the time for the calculation of the manifold itself, this is negligible. On the other hand the storage requirement for the ILDM is reduced dramatically if the polynomial approximation is used. The table with the old storage scheme needs about 15 Mbytes storage, whereas the new table does only occupy about 80 kbytes.

The results presented above show the improvement of the new scheme compared with our previously used storage scheme [16]. In order to further verify the approach and its implementation in CFD-codes, we performed laminar flat flame calculations for a stoichiometric hydrogen-oxygen system (cf. [17]). In the flat flame code the table look-up procedure has been replaced by a subroutine evaluating the polynomial approximations. Calculations of flame profiles were performed for detailed chemistry as well as for ILDM-reduced chemistry using both storage schemes. The computation time is reduced drastically by using ILDM-reduced chemistry for both storage schemes. Compared to the old tabulation the new polynomial tabulation scheme does not affect the computation time significantly. Figures 7 - 9 show temperature and various species profiles in the flame. Temperature, major species like  $H_2$  and  $H_2O$ , and minor species like O, OH and H are reproduced very well by the reduced schemes. There is no significant difference between both storage schemes, which is very promising, because on the other hand the storage requirement is reduced by a factor of 200 using the new polynomial approximation.

## 4 Conclusions

In most practical reacting flow calculations the direct use of detailed chemistry is computationally prohibitive. Thus, reduced chemical kinetics schemes are devised, which allow to describe the chemical system in terms of a small number of reaction progress variables, and very often the information on the chemical kinetics (e.g., reaction rates) is calculated beforehand and stored for the CFD-calculation. We have developed a storage scheme based on orthogonal polynomials. Instead of using a locally refined tabulation grid together with

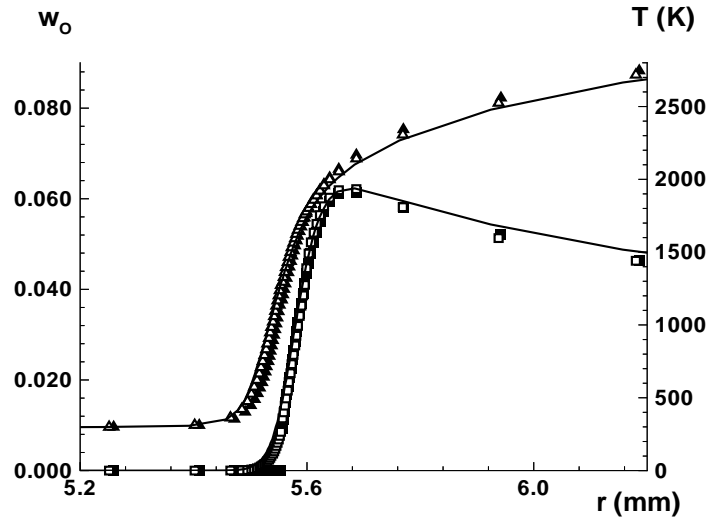


Figure 7: Profiles of temperature ( $\Delta$ ) and O-radicals ( $\square$ ) in a premixed laminar  $\text{H}_2\text{-O}_2$  flame. The lines denote computation with detailed and the symbols with reduced chemistry. (full symbols: Standard look-up table, empty symbols: New polynomial table).

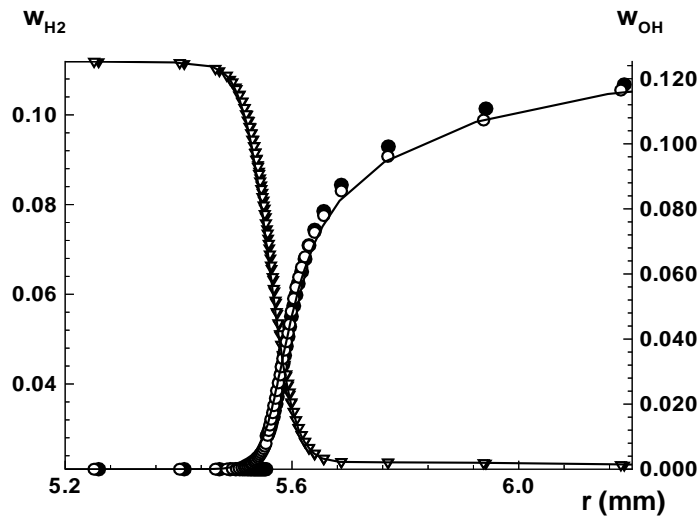


Figure 8: Profiles of  $\text{H}_2$  ( $\nabla$ ) and OH-radicals ( $\circ$ ) in a premixed laminar  $\text{H}_2\text{-O}_2$  flame. The lines denote computation with detailed and the symbols with reduced chemistry. (full symbols: Standard look-up table, empty symbols: New polynomial table).

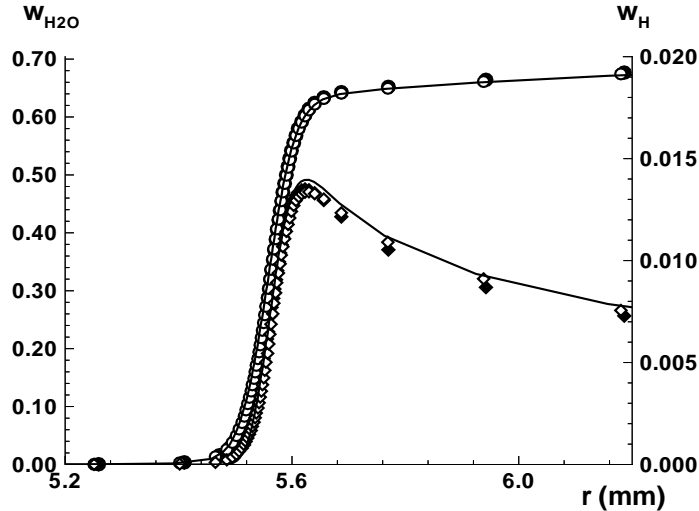


Figure 9: Profiles of  $\text{H}_2\text{O}$  ( $\circ$ ) and  $\text{H}$ -radicals ( $\diamond$ ) in a premixed laminar  $\text{H}_2\text{-O}_2$  flame. The lines denote computation with detailed and the symbols with reduced chemistry. (full symbols: Standard look-up table, empty symbols: New polynomial table).

multi-linear interpolation within the grid cells [16], we divide the domain into a small number of coarse cells and use polynomial approximations within these cells. Special methods assure that the polynomial approximations are not only continuous within the coarse cells, but all over the domain. The storage requirement is reduced considerably. In order to verify the approach, calculations of laminar premixed flat flame calculations have been performed for a stoichiometric hydrogen-oxygen system using both detailed and ILDM-reduced chemistry. In this specific example the storage requirement is reduced by a factor of 200. However, the storage procedure is not restricted to the use together with ILDM-reduced chemistry. Other applications of storage schemes are, e.g., the storage of pre-integrated reaction rates for turbulent flame calculations [28] or the storage of laminar flamelet libraries [29]. For such applications the polynomial storage scheme might be used, too.

## 5 Acknowledgments

The authors would like to thank T. Turanyi leading their attention on the advantages of storage schemes based on orthogonal polynomials. Financial support by the CEC (in the frame of the BRITE/EURAM-Project) and the *BMFT* (in the frame of the TECFLAM-Project) is gratefully acknowledged.

## References

- [1] J. Warnatz. 24th Symposium (International) on Combustion. The Combustion Institute, Pittsburgh, 1992.
- [2] U. Maas and J. Warnatz. *IMPACT Comp. Sci. Eng.*, 1:394, 1989.
- [3] J. Warnatz, U. Maas, and R. W. Dibble. *Combustion*. Springer-Verlag Berlin Heidelberg New York, 1996.

- [4] S. B. Pope. 23rd Symposium (International) on Combustion. The Combustion Institute, Pittsburgh, 1990.
- [5] N. Peters. 21st Symposium (International) on Combustion. The Combustion Institute, Pittsburgh, 1986.
- [6] P. A. Libby and F. A. Williams (eds.). *Turbulent Reactive Flows*. Springer, New York, 1980.
- [7] C. Chevalier. *Entwicklung eines detaillierten Reaktionsmechanismus zur Modellierung der Verbrennungsprozesse von Kohlenwasserstoffen bei Hoch- und Niedertemperaturbedingungen*. PhD thesis, Institut für Technische Verbrennung, Universität Stuttgart, 1993.
- [8] M. Bodenstein. *Z. Phys. Chem.*, 57:168, 1906.
- [9] N. Peters and B. Rogg. *Reduced Kinetic Mechanisms for Applications in Combustion Systems*. Springer, Berlin, 1993.
- [10] J. C. Keck. 22nd Symposium (International) on Combustion. The Combustion Institute, Pittsburgh, 1988.
- [11] S. H. Lam and D. A. Goussis. 22nd Symposium (International) on Combustion. The Combustion Institute, Pittsburgh, 1988.
- [12] S. H. Lam and D. A. Goussis. Conventional asymptotics and computational singular perturbation for simplified kinetics modelling. Technical report, Princeton University, USA. Technical Report 1864(a)-MAE, 1990.
- [13] F. C. Christo, A. R. Masri, E. M. Nebot, and T. Turanyi. *Utilising Artificial Neural Network and Re-pro-Modelling in Turbulent Combustion*. Proc. of the IEEE Symposium on Artificial Neural Networks, , Perth, 1995.
- [14] P. Deuffhard and J. Heroth. Dynamic dimension reduction in ODE models. Technical report, Konrad-Zuse-Zentrum für Informationstechnik Berlin, PreprintSC95-29, 1995.
- [15] U. Maas and S. B. Pope. Simplifying chemical kinetics: Intrinsic low-dimensional manifolds in composition space. *Combustion and Flame*, 88:239–264, 1992.
- [16] U. Maas and S. B. Pope. 24th Symposium (International) on Combustion. The Combustion Institute, Pittsburgh, 1992.
- [17] U. Maas and S. B. Pope. *Laminar Flame Calculations using Simplified Chemical Kinetics Based on Intrinsic Low-Dimensional Manifolds*. 25th Symposium (International) on Combustion. The Combustion Institute, Pittsburgh, 1994.
- [18] M. D. Smooke (ed.). *Reduced Kinetic Mechanisms and Asymptotic Approximations for Methane-Air Flames*. Lecture Notes in Physics 384, Springer, Berlin, Heidelberg, New York, 1991.
- [19] A. S. Tomlin, T. Turanyi, and M. J. Pilling. Mathematical tools for the construction, investigation and reduction of combustion mechanisms. In M. J. Pilling, editor, *Oxidation Kinetics and Autoignition of Hydrocarbons*. Elsevier, in press.

- [20] U. Maas. Coupling of chemical reaction with flow and molecular transport. *Applications of Mathematics*, 3:249–266, 1995.
- [21] U. Maas. *Automatische Reduktion von Reaktionsmechanismen zur Simulation reaktiver Strömungen*. Habilitation Thesis, Institut für Technische Verbrennung, Universität Stuttgart, 1993.
- [22] D. Schmidt, U. Maas, and J. Warnatz. *Simplifying Chemical Kinetics for the Simulation of Hypersonic Flows using Intrinsic Low-Dimensional Manifolds*. Proc. of the 5<sup>th</sup> International Symposium on Computational Fluid Dynamics, Sendai, Japan, 1993.
- [23] D. Schmidt, U. Maas, J. Segatz, U. Riedel, and J. Warnatz. Simulation of laminar methane-air flames using automatically simplified chemical kinetics. *Comb. Sci. Tech.*, Accepted for Publication.
- [24] U. Riedel, D. Schmidt, U. Maas, and J. Warnatz. *Laminar Flame Calculations Based on Automatically Simplified Chemical Kinetics*. Proc. of the 35<sup>th</sup> Eurotherm Seminar, Compact Fired Heating Systems, Leuven, Belgium, 1994.
- [25] T. Turanyi. Parameterization of reaction mechanisms using orthonormal polynomials. *Computers Chem.*, 18:45–54, 1994.
- [26] B. Yang and S. B. Pope. *A Tree Method for Treating Chemical Reactions in PDF Calculations of Turbulent Combustion*. Proc. 6th International Conference on Numerical Combustion, New Orleans, 1996.
- [27] I.N. Bronstein und K.A. Semendjajew. *Taschenbuch der Mathematik*. BSB B.G. Teubner Verlagsgesellschaft, Leipzig, 1979.
- [28] A. T. Norris and S. B. Pope. Modeling of extinction in turbulent diffusion flames by the velocity-dissipation-composition pdf method. *Combustion and Flame*, 100:211–220, 1995.
- [29] J. Göttgens, F. Mauss, and N. Peters. 24th Symposium (International) on Combustion. The Combustion Institute, Pittsburgh, 1992.